Mueller tensor approach for nonlinear optics in turbid media

James R. W. Ulcickas, Fengyuan Deng, Changqin Ding, Garth J. Simpson

James R. W. Ulcickas, Fengyuan Deng, Changqin Ding, Garth J. Simpson, "Mueller tensor approach for nonlinear optics in turbid media," Proc. SPIE 10498, Multiphoton Microscopy in the Biomedical Sciences XVIII, 1049834 (23 February 2018); doi: 10.1117/12.2289999

SPIE.

Event: SPIE BiOS, 2018, San Francisco, California, United States

Mueller tensor approach for nonlinear optics in turbid media

James R.W. Ulcickas, Fengyuang Deng, Changqing Ding, Garth J. Simpson
Department of Chemistry, Purdue University, 560 Oval Drive, West Lafayette, Indiana, USA 47907

ABSTRACT

As plane-polarized light propagates through a turbid medium, scattering alters the phase and polarization differently in different locations. The corresponding depolarization of the beam complicates recovery of the rich information content contained within the polarization-dependence of second harmonic generation (SHG) microscopy. A theoretical framework connecting Jones and Stokes formalisms for describing optical polarization allows prediction of the polarization-dependent SHG produced from "ballistic", but depolarized incident light. Measurements with collagen-rich tissue sections support the predictions of the framework. Partially polarized SHG produced from a depolarized source enabled recovery of local orientation distribution for collagen and local tensor information. Bridging the gap between SHG instigated by fully depolarized light and partially polarized light more common to practical turbid systems, a method for predicting local nonlinear optical susceptibility tensor elements was developed and applied to collagen in thick sections. Recovered values for the tensor element ratio ρ are in good agreement with previous results for thin tissue and literature reports.

Keywords: Second harmonic generation, microscopy, polarization analysis, collagen, turbid media, Mueller tensors, tissue imaging, unpolarized

1. INTRODUCTION

Second harmonic generation (SHG) has been utilized for many years for highly specific detection of ordered structures, owing to the strict symmetry requirements of the process. The requirement for non-centrosymmetric structure has made SHG imaging a powerful tool for biological structures such as collagen and myosin.[1] Further utility is granted through the process' quadratic dependence upon power, resulting in tighter axial confinement of the image plane in microscopy applications and the absence of significant out-of-plane contributions, even in turbid media. In addition, SHG affords the use of near infrared laser sources, enabling minimal absorptive losses of the fundamental by operating in the optical window. These advantages are powerful, but SHG as a tool has inherently limited information content due to the lack of spectral information in the measurement; intensity is the only observable. To further improve the informational capacity of SHG measurements, much work has been done to utilize the polarization dependence of the process.[2-4] SHG activity is governed by the complex valued nonlinear optical susceptibility, a second rank tensor which provides probable phase and amplitude of scattered photons given phase and amplitude of two coherent photons passing through the medium.[5] This tensor contains valuable structural information related to the symmetry of the SHG active species. Despite this potential utility, polarization dependent nonlinear optics can be challenging in many practical systems due to partial or complete depolarization of the fundamental beam from scattering. This work further advances efforts to employ polarization dependent nonlinear optics in turbid media by i) development of a theoretical framework capable of expressing the Mueller tensor describing SHG from partially polarized light in terms of the simpler and more familiar Jones/Cartesian tensor, ii) application of a depolarized fundamental for polarization analysis of the SHG, producing experimental data in good agreement with theory, and iii) implementation of a new Mueller tensor based approach to predict elements of the local nonlinear optical (NLO) susceptibility tensor $\chi_l^{(2)}$ for collagen fibers embedded in 40 μm thick tissue.

Implementation of polarization dependent nonlinear optical imaging in complex media has been a challenge since the field's inception. In tissue analysis, early efforts attempted to minimize the effects of scattering and birefringence by only working on thin sections. In 2009 Nadiarnykh and Campagnola were able to remove scattering contributions from tissue sections as thick as 100 μm by employing optical clearing techniques, reducing the impact of scattering on the polarization

Multiphoton Microscopy in the Biomedical Sciences XVIII, edited by Ammasi Periasamy, Peter T. C. So, Karsten König, Xiaoliang S. Xie, Proc. of SPIE Vol. 10498, 1049834

of SHG.[6] Since then, more effort has been placed on methods to recover polarization-dependent information without further treating the sample. Recently, de Aguiar et al. reported a method for polarization-dependent SHG whereby wavefront shaping was utilized to correct for scattering during propagation to the focal plane and conserve polarization of the fundamental.[7] Others have pursued a theoretical approach to turbid media NLO, expanding theoretical frameworks developed for linear optics to the nonlinear. Barzda and coworkers have proposed a method known as double stokes double Stokes Mueller polarimetry, which relies on the construction of the double Mueller matrix, analogous to the Mueller matrix for linear optics, to predict outgoing SHG given incident Stokes vectors describing the polarization state of light.[8] Simpson proposed a similar framework in 2016, opting for the use of Mueller tensors, analogous to the Jones tensors used for describing NLO in the regime of well-defined polarization.[9]

This work reports a new method to recover local-frame tensor information for SHG active materials embedded in turbid media, with application to collagen structures. To achieve this new method, a preliminary experimental approach was developed to first verify the Mueller-Stokes theoretical framework described in reference 9.[9] A microretarder array (DPP25-B, Thorlabs) was employed to depolarize light prior to penetrating the turbid thick tissue section. By beginning with a fully depolarized light source it is expected that any birefringence or scattering within the tissue will not significantly perturb the polarization state of the light as it propagates to the focal plane. Recovered values for tensor element ratio ρ and orientation angles of collagen were in reasonable agreement with previous experiment and image analysis approaches. Building off of the success of the depolarized approach, a method utilizing the measurement of the Stokes vector for both the second harmonic and the fundamental was developed. This approach utilizes the measured Stokes vectors to fit for the tensor element products determining Stokes frame SHG, enabling the recovery of information such as sample orientation and tensor element magnitudes.

2. THEORY

2.1 Introduction to the Stokes-Mueller Formalism

In classical optics, the Jones-matrix formalism is used to describe the polarization of non-depolarized light in terms of the relative electric field components. The Jones vector is a two-element complex vector with unit amplitude whose elements correspond to orthogonal field axes, as shown in (1) below with field axes oriented at the horizontal and vertical planes. Multiplying the Jones vector by an appropriately constructed Jones matrix can track the changes in polarization that occur as light propagates through, for example, a microscope. Equation 1 below demonstrates the form of the Jones vector and its propagation through a linear optical element represented by the Jones matrix J.

$$\vec{e}_{out} = J \cdot \vec{e}_{in} = J \cdot \begin{bmatrix} e_H \\ e_V \end{bmatrix}_{in} \tag{1}$$

This framework provides a convenient method for tracking polarization change of light as it propagates through optical elements and is trivially extended to nonlinear optics. In second order nonlinear optics such as SHG or SFG, the 2x2 Jones matrix is replaced by a 2x2x2 Jones tensor, which maps the two incident polarization states into a single output polarization state.

The simplicity of the Jones framework is its greatest asset for many applications. However, when pristine polarization states are not guaranteed, the Jones architecture proves insufficient. Instead a more general Stokes framework can be employed, again relying on vector-valued representations of polarization state with optical elements being represented by matrices and nonlinear-optical constructs higher order tensors. Equation 2 below defines the Stokes vector as the Kronecker product ($\otimes$) of the incident Jones vector with its complex conjugate, multiplied by the transfer matrix A.

$$\vec{s} = \begin{pmatrix} I_H + I_V \\ I_H - I_V \\ I_{+45} - I_{-45} \\ I_R - I_L \end{pmatrix} = \begin{bmatrix} 1 & 0 & 0 & 1 \\ 1 & 0 & 0 & -1 \\ 0 & 1 & 1 & 0 \\ 0 & i & -i & 0 \end{bmatrix} \cdot \begin{pmatrix} \vec{e}_H^* \vec{e}_H \\ \vec{e}_H^* \vec{e}_V \\ \vec{e}_V^* \vec{e}_H \\ \vec{e}_V^* \vec{e}_V \end{pmatrix} = A \cdot \left(\vec{e}^* \otimes \vec{e} \right) \tag{2}$$

In much the same way, Mueller matrices and Mueller tensors for propagating polarization through Stokes vectors can be constructed from their parent Jones matrices using the transfer matrix *A*. Equation (3) below denotes the construction of a Mueller matrix M from the Jones matrix J representing the same optic.

$$\vec{s}_{out} = A \cdot \left(J^* \otimes J \right) \cdot A^{-1} \cdot \vec{s}_{in} = M \cdot \vec{s}_{in} \tag{3}$$

Equation (4) below shows the construction of a rank two Mueller tensor $M^{(2)}$ from the Jones-frame tensor $\chi_J^{(2)}$ and transfer matrix *A*. Note that $M^{(2)}$ is a 4x4x4 tensor, containing a total of 64 elements, of which 36 may be unique for SHG.[10] A more in-depth review of this mathematical framework can be found in Ref 9.[9]

$$M^{(2)} = A \cdot \left(\chi_J^{(2)*} \otimes \chi_J^{(2)} \right) : A^{-1} A^{-1} \tag{4}$$

Utilizing the Stokes vector, a fully depolarized state of light may be defined as the vector where only the first element of $\vec{s}$ is nonzero. Partially depolarized Stokes vectors can often be approximated as a linear combination of purely polarized and fully depolarized components. As a direct consequence, a sample probed with depolarized light radiates SHG solely from four unique elements of the $M^{(2)}$ tensor. Equation 4 below illustrates the stokes vector of the SHG to a linear combination of polarized and depolarized light and to the contributing elements of the NLO susceptibility. The contributing elements of $M^{(2)}$ are written with binary indices; this enables conversion between the tensor and vectorized form of the $M^{(2)}$ tensor, which facilitates linear fitting procedures and simplifies algebra.

$$\begin{bmatrix} s_0 \\ s_1 \\ s_2 \\ s_3 \end{bmatrix}_{obj}^{2\omega} = \alpha \cdot \vec{s}_{depol}^{2\omega} + (1-\alpha) \cdot \vec{s}_{pol}^{2\omega} = \alpha \cdot \begin{bmatrix} M_{000} \\ M_{100} \\ M_{200} \\ M_{300} \end{bmatrix}_{depol} + (1-\alpha) \cdot M_{pol}^{(2)} : \vec{s}_{in}^{\omega} \vec{s}_{in}^{\omega} \tag{5}$$

In the general case, the NLO susceptibility of the sample is oriented in a reference frame separate from the measurement frame. For convenience, we will consider the light incident to the sample to be oriented with respect to the detection optics and refer to this reference frame as the laboratory frame. The tensor product of the laboratory frame NLO susceptibility $\chi_L^{(2)}$ with the two incident fields produces the outgoing polarization. The experimentally relevant tensor, however, exists in the local frame as $\chi_l^{(2)}$. Relating the correct outgoing polarization to the local frame tensor can be achieved by rotating the incident field to the frame of the local tensor, followed by rotation of the outgoing field vector to the laboratory frame as shown in Equation (6) below.

$$\vec{e}^{2\omega} = \chi_L^{(2)} : \vec{e}^{\omega} \vec{e}^{\omega} = R_{-\phi} \chi_l^{(2)} : \left(R_\phi \vec{e}^{\omega} \right) \left(R_\phi \vec{e}^{\omega} \right) \tag{6}$$

In an analogous structure to equation (6), the Stokes-Mueller framework instead takes the tensor product of the laboratory frame incident Stokes vectors with the laboratory frame Mueller tensor. Equation (7) shows Stokes-frame rotation matrices $\mathcal{R}_\phi$ serve to rotate the incident and outgoing Stokes vectors to and from the local frame, respectively.

$$\vec{S}^{2\omega} = M_L^{(2)} : \vec{S}^{\omega}\vec{S}^{\omega} = \mathcal{R}_{-\phi} M_l^{(2)} : \left(\mathcal{R}_\phi \vec{S}^{\omega}\right)\left(\mathcal{R}_\phi \vec{S}^{\omega}\right) \tag{7}$$

2.2 SHG From Depolarized Light

The mathematical framework above allows prediction of the polarization-dependent SHG produced from unpolarized light within the context of the simpler Jones framework. Previous studies designed to test the validity of these predictions showed excellent agreement between theory and experiments for both Z-cut quartz and thin sections of collagen.[11] Experimentally, this was achieved by placing a depolarizing optic (microretarding array) in the Fourier plane before the objective, such that the cross-sectional area contains varying polarization states as a function of position. When focused to a point through the objective the focal volume is probed by many polarizations at once, effectively depolarizing the beam. Briefly, the mathematics determining expected SHG polarization for the specific case of collagen will be described.

As introduced in equation (5), all scattered SHG for a depolarized fundamental is contributed from only 4 unique Mueller tensor elements. The origin of these tensor elements can be traced back to the underlying Jones tensor, as indicated by equation (4). Explicitly evaluating the contribution of Jones tensor elements to the resulting tensor yields equation (8) below.

$$\begin{bmatrix} s_0 \\ s_1 \\ s_2 \\ s_3 \end{bmatrix}^{2\omega} = \tfrac{1}{4}\begin{bmatrix} 1 & 0 & 0 & 1 \\ 1 & 0 & 0 & -1 \\ 0 & 1 & 1 & 0 \\ 0 & i & -i & 0 \end{bmatrix}\begin{bmatrix} \chi^*_{000}\chi_{000} + \chi^*_{001}\chi_{001} + \chi^*_{010}\chi_{010} + \chi^*_{011}\chi_{011} \\ \chi^*_{000}\chi_{100} + \chi^*_{001}\chi_{101} + \chi^*_{010}\chi_{110} + \chi^*_{011}\chi_{111} \\ \chi^*_{100}\chi_{000} + \chi^*_{101}\chi_{001} + \chi^*_{110}\chi_{010} + \chi^*_{111}\chi_{011} \\ \chi^*_{100}\chi_{100} + \chi^*_{101}\chi_{101} + \chi^*_{110}\chi_{110} + \chi^*_{111}\chi_{111} \end{bmatrix} \tag{8}$$

The above equation is written in the reference frame of the measurement, or the laboratory frame, in which all eight combinations of Jones tensor elements will generally be nonzero and unique. For collagen in the Jones frame oriented with the unique fiber axis coparallel with the local vertical axis, the nonzero elements within the local frame are significantly reduced to just three: χ_{VVV} , χ_{VHH} , and $\chi_{HHV} = \chi_{HVH}$. Relating this reference frame to the laboratory frame in equations (5) and (8) can be achieved through the use of rotation matrices corresponding to reference frame rotations by an angle ϕ, a simplified form of which is shown below in equation (9).

$$\begin{bmatrix} s_0 \\ s_1 \\ s_2 \\ s_3 \end{bmatrix}^{2\omega} = \tfrac{1}{4}\begin{bmatrix} 1 & 1 & 1 \\ \cos(2\phi) & \cos(2\phi) & -\cos(2\phi) \\ -\sin(2\phi) & -\sin(2\phi) & \sin(2\phi) \\ 0 & 0 & 0 \end{bmatrix}\begin{bmatrix} \left|\chi_{VVV}\right|^2 \\ \left|\chi_{VHH}\right|^2 \\ 2\left|\chi_{HHV}\right|^2 \end{bmatrix} \tag{9}$$

Utilizing the approximation $\left|\chi_{VHH}\right| \cong \left|\chi_{HHV}\right|$ consistent with experimental studies of collagen and multiplying by $\left|\chi_{VHH}\right| / \left|\chi_{VHH}\right|$ the full equation may be put in terms of the ratio $\rho = \left|\chi_{VVV} / \chi_{VHH}\right|$.[11-13] Lastly, the detected intensity as a function of analyzing polarizer angle is expressed in equation (10) below. A nonlinear fit to this equation from a data set consisting of multiple rotation angles for the detection polarizer yields values for ρ and for ϕ, the orientation of collagen at each given pixel.

$$I^{2\omega}\left(\phi_{pol}\right) = \frac{C}{8}\left[\left(\left|\rho\right|^2 + 3\right) + \left(\left|\rho\right|^2 - 1\right)\cos\left(2\phi_{pol} - 2\phi\right)\right] \tag{10}$$

3. METHODS

3.1 Microscopy

Imaging was conducted on a custom-built microscope utilizing an 80 MHz 100 fs Mai Tai Ti:Sapphire laser (SpectraPhysics) operating at 800nm as source. Beam-scanning microscopy was performed by pairing a resonant mirror operating at 8.8kHz (EOPC) with a galvanometer mirror synced such that 512 repetitions of the resonant mirror path occur for one ramp from the galvo mirror. The beam is then expanded to overfill the back of the objective and focused through a 10x 0.3 NA objective (Nikon). Scattered and transmitted light is collected by a 0.3 NA 10x condenser, and passed through a 4f configuration to deliver collimated light to the detection optics. Following collection through the condenser, light passes through a quarter wave plate (400nm, Thorlabs) and a broadband wire grid depolarizer (0.2-2um, Thorlabs) placed in precision automated rotation stages (Universal Motion Controller, ESP300 and rotation mount, SR50CC, Newport). A dichroic mirror reflects the frequency doubled light, passing through a band pass filter (HQ 400/20m-2p Chroma Technology) and is detected on a photomultiplier tube (PMT, Hamamatsu H12310-40). The fundamental passes through the dichroic and is detected on a photodiode (DET10, Thorlabs). Figure 1 below demonstrates the setup.

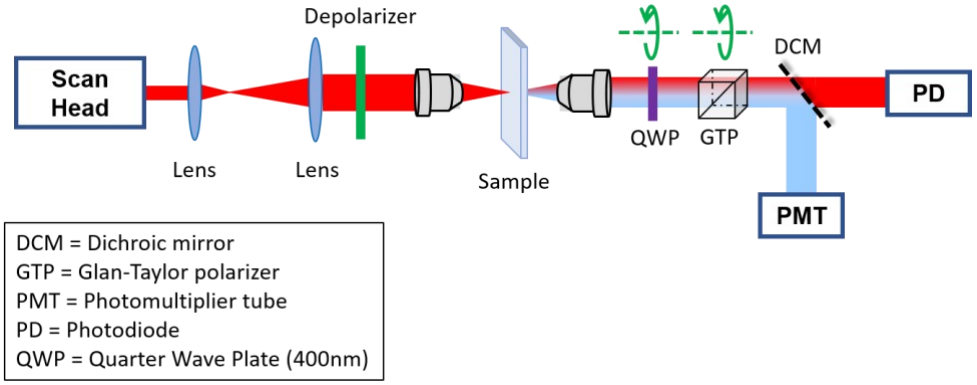

Figure 1. Instrument schematic from the scan head to detection optics. The depolarizer and QWP are removable optics from this beam path; Stokes measurements of section 4.3 were made without the depolarizer while depolarized SHG measurements of section 4.2 were conducted with the QWP removed.

Stokes measurement experiments were carried out with an electro-optic modulator (Conoptics) placed in the beam path prior to the scan head, operating at 8MHz. This enables polarization modulation with a period of ten laser pulses, allowing the construction of ten separate polarization-modulated images acquired simultaneously.

To ensure that negligible depolarization of the second harmonic occurred, the laser was first focused upon the sample slide, then translated to find a region that was SHG active at that focal plane. Minor focus adjustments were then made to improve signal.

3.2 Stokes Ellipsometric Microscopy – Data Analysis

From the definition of the Stokes vector shown in Equation (2) it is clear that the Stokes vector can be measured directly by separately measuring I_H, I_V, I_{+45}, I_{-45}, I_R and I_L. These measurements may be obtained in sequence by rotating a quarter wave plate paired with a polarizer prior to detection optics. Using the Jones-Stokes formalism described in section 2.1, the effects of all optics post-sample can be accounted for and utilized to directly measure the Stokes vector of light produced after the sample. Equation (11) below describes the effect of post-sample optics on the light leaving the sample plane and entering the detection arm ($\vec{S}_{out}$) in the Stokes framework. The matrices *R* represent Stokes-frame rotation matrices, used to rotate the light from the laboratory frame to the local orientation of the quarter wave plate (M_{WP}) and then subsequently rotate the light to the frame of the detection polarizer (M_{pol}). Lastly, the integrated intensity is detected and so only the first element of the resulting Stokes vector is measured.

$$I_{\text{det}} = \begin{bmatrix} 1 \\ 0 \\ 0 \\ 0 \end{bmatrix} \cdot M_{pol} \cdot R(\phi_{pol}) \cdot R(-\gamma) \cdot M_{WP} \cdot R(\gamma) \cdot \vec{S}_{out} = \mathbf{F} \cdot \vec{S}_{out} \tag{11}$$

Since the elements of the Stokes vector are all linear combinations of intensities, a fitting matrix can be constructed to recover the Stokes vector of detected light, given several orientations of M_{WP} and M_{pol}. Defining the set of polarization transfer matrices as a single matrix $\mathbf{F}$ enables inversion by multiplying by $\mathbf{F}^T$, and for a sufficiently overdetermined data set the Stokes vector at the sample plane can be recovered. Typical experiments utilize angles for the polarizer of -45, 0, +45, and +90 degrees, enabling direct detection of the first three Stokes vector elements. A 400nm QWP is rotated from its fast axis at 0, through to 22.5 and 45 degrees for each angle of the polarizer, providing 12 measurements at each pixel.

The utility of this linear fitting approach is most greatly apparent for applications in which we wish to measure the Stokes vector of both the fundamental beam as well as the SHG. By replacing the matrix M_{WP} with an arbitrary retarder matrix (conveniently, instead of half wave retardance quarter wave retardance is achieved for the 800nm fundamental) recovery of the full Stokes vector of the fundamental is possible despite the lack of an 800nm QWP. This was verified by sending a variety of polarization states known by calibration of a pair of half and quarter waveplates through the microscope and recovery of the expected Stokes vector.

3.3 Sample Preparation

Mouse tail samples were obtained from Prof. Philip Low (Purdue University, West Lafayette, IN) and fixed in 10% neutral buffered formaline. The tail was subsequently decalcified in solution of Formical-4 (StatLab) for 5 hours, then placed in a 15% sucrose solution in PBS overnight, followed by a 30% sucrose solution in PBS overnight for cryoprotection. The tails were then embedded in OCT and frozen using isopentane chilled with liquid nitrogen. Tissue sections were taken from the central region of the tail, cut longitudinally using a Leica CM 1860 cryostat.

4. RESULTS AND DISCUSSION

4.1 Demonstration of depolarization from turbid media

To confirm the prepared 40 µm thick tissue slices induce partial depolarization, a simple polarizer rotation experiment was conducted. In this experiment, the analyzer was rotated in 3 degree increments for a total of 180 degrees. Figure 2 below shows the integrated laser transmittance image for all polarizations (A) and several plots of intensity integrated over the shown colored boxes (B).

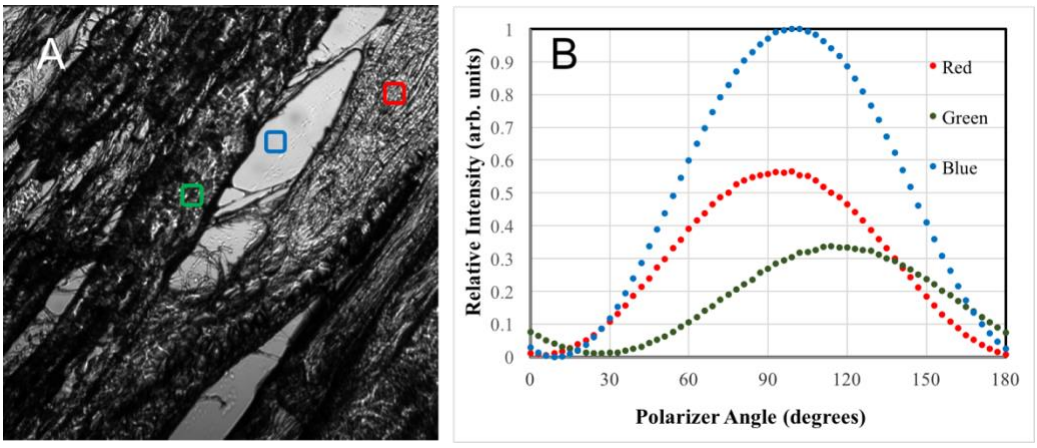

Figure 2. A) 40 µm thick tissue image integrated over 60 rotation angles for detection polarizer. Colored squares indicate regions that are plotted in B). B shows the intensity as a function of rotation angle with intensities normalized to the maximum in region containing no tissue (blue). There is evidence of both phase shift and amplitude modulation for the green and red regions.

Figure 2 above shows significant birefringence and scattering for light propagating through 40 μm thick tissue, with a 39% loss in extinction ratio for the red area and a 59% reduction in the green . It is posited that the phase shift observed in the red and green traces of figure 2B is associated with scattering and birefringence, while the change in amplitude of modulation is primarily due to scattered light not collected by the condenser. In the case of perfect half wave retardance, where circular polarization is created, it is expected that rotation of a linear polarizer will produce equal intensity at all rotation angles for the analyzer. As the degree of retardance, and thereby birefringence of the sample, increases toward a maximum at half wave retardance, the overall extinction ratio and amplitude of modulation is expected to decrease. However, it must be noted that in the case of pure birefringence inducing ellipticity, it is expected that the minimum observed signal should also increase, such that intensity is detected at every angle of the polarizer. In figure 2 above the minimum value for each trace does not vary significantly from zero. Nevertheless, birefringence may produce polarization ration effects consistent with this phase shift. Furthermore, when considering only the effect of scattering, it is expected that interconversion between the H and V polarizations will effectively rotate the plane of polarization of light passing through the sample. This will ultimately manifest as a phase shift in the plot shown in figure 2B.

4.2 Recovering Local Frame Tensor Information Through Turbid Media

For depolarized SHG experiments, a similar data acquisition approach as in 4.1 was utilized. The depolarizing optic was placed in the Fourier plane immediately prior to the objective and a sequence of images was acquired with varying detection polarizer angles. The resulting data set was stacked as a vector and a nonlinear fit was performed to recover ρ and ϕ on a per-pixel basis according to equation (10). Figure 3 below shows the recovered orientation map (A) and ρ map (B).

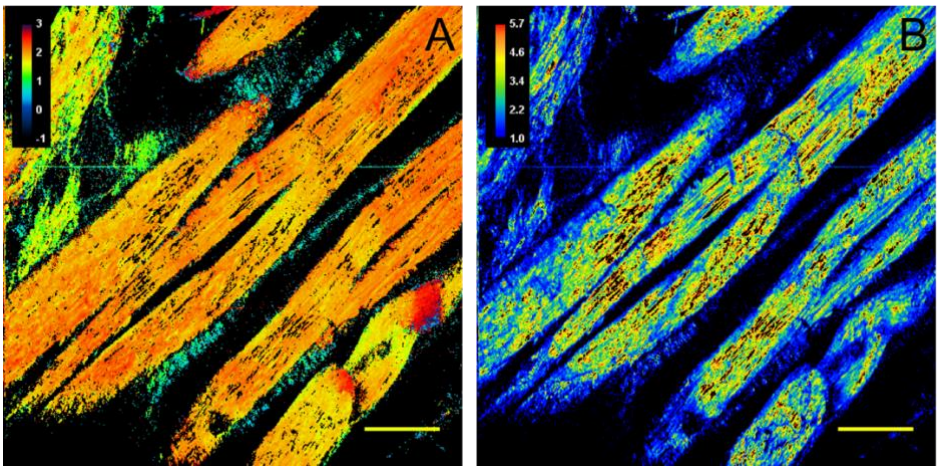

Figure 3. A) Orientation map of primary collagen fiber axis, ie; angle ϕ defined from 0 to π. Consistent change in coloration as a function of the angle of the larger fiber structure is observed. Background is set to black as only regions in the FoV with greater than 1% of the maximum SHG signal are evaluated for ρ and ϕ. B) ρ map for collagen fibers. Mean measured ρ is 2.55, greater than previous reports of the method with thin tissue. It is noted that regions of more intense SHG activity show larger absolute magnitudes for ρ.

The mean recovered ρ for the above data set is 2.55, larger than the value of 1.7 obtained from thin tissue analysis. One potential explanation for this discrepancy is that the SHG does not occur precisely at the edge of the thick sample, and thus scattering and birefringence may affect the polarization of the second harmonic light. Alternatively, the mean of the ratio could be biased by measurement noise; low values in the denominator from Poisson noise can result in large values in the ratio that are not balanced by correspondingly large values in the denominator. The distribution of voltage from the PMT can be approximated as a convolution of the Poisson distribution of photons with the lognormal distribution of the PMT gain. Simulations confirmed that the ratio of two such distributions produces a data set with the mean artificially biased large. It is worth emphasizing that the ratio obtained in the preceding analysis is recovered using fully depolarized light and is therefore entirely immune from artifacts related to depolarization or birefringence within the sample.

Nevertheless, the values obtained are in generally good agreement with those produced for pristine samples measured with purely pure polarizations. The depolarizer-based approach provides critical proof-of-concept data for validating the Mueller-Stokes model, through which local frame tensor information is recovered for collagen embedded deeply within a 40 μm thick section of highly birefringent and turbid tissue; a comparable feat has not yet been reported without optical clearing or wavefront shaping. This mathematical framework is also the first to quantitatively describe and predict the polarization-dependent SHG expected when driven by an unpolarized fundamental beam in terms of the simple Jones tensor framework.

4.3 Mueller Tensor Approach

The theoretical framework described in section 2 enabled the use of a more holistic approach to describe SHG produced by partially polarized light. For the specific case of collagen, we can make several approximations regarding the nonzero unique elements of the local frame tensor $\chi_l^{(2)}$. In the local frame of collagen, with the primary unique axis of the fiber defined as the V axis, the nonzero elements are χ_{VVV}, χ_{VHH}, $\chi_{HHV} = \chi_{HVH}$. Previous studies have suggested the approximation $\chi_{VHH} = \chi_{HHV}$ to be well founded, reducing the total number of unique nonzero elements in the local frame tensor to 2.[3, 12] Equation (7) can be rewritten in the vectorized notation, suitable for linear inversion through a vectorization protocol described in ref 9.[9]

There are two key aspects for data analysis utilizing this method of linear inversion. First, for the matrix to be sufficiently overdetermined to invert, it is necessary to obtain several different Stokes vectors for the fundamental and second harmonic leaving the focal plane at each pixel. This can be achieved by manual rotation of a wave plate prior to the sample so that multiple polarizations are sampled; our approach instead utilizes an electro-optic modulator as described in section 3.1, stacking the Stokes vectors for each unique incident polarization state. The second key detail is that the orientation of collagen at each pixel must be known *a priori* in order to evaluate the matrix **R**. The azimuthal angle can either be determined iteratively as has been demonstrated in prior work, or by independent image analysis using contextual cues such as performed using the ImageJ plug-in OrientationJ.[14, 15] As these two approaches have been found to yield excellent agreement in previous studies of thin tissue, [11] the azimuthal angles produced by OrientationJ were assumed in the present treatment to be reliable, with polarization analysis selectively performed to recover the local-frame tensor elements. Data analysis recovers three images, corresponding to the amplitude of $|\chi_{VVV}|^2$, $|\chi_{VHH}|^2$ and the cross term. The magnitude of the tensor element ratio ρ is determined by taking the square root of the ratio $|\chi_{VVV}|^2 / |\chi_{VHH}|^2$, with the sign recovered from the cross-term. Figure 4 below demonstrates the recovered ρ map and the distribution of ρ values.

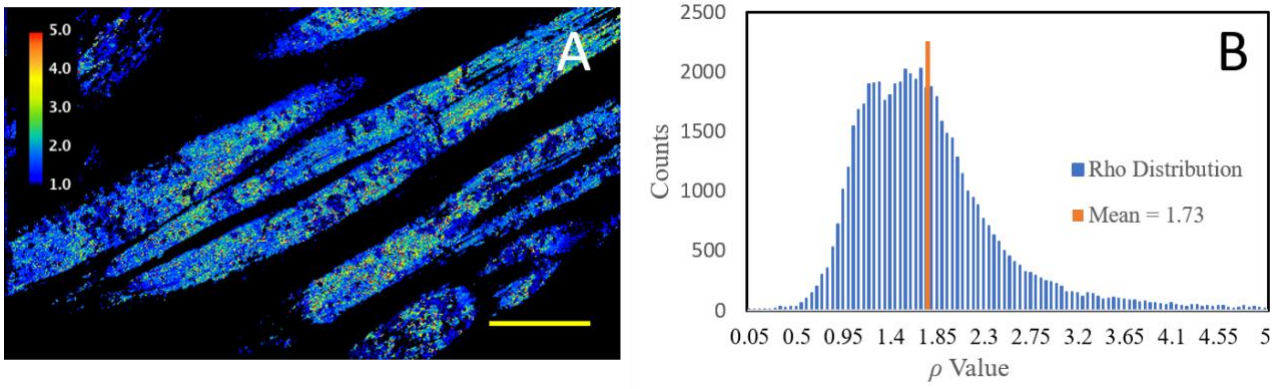

Figure 4. A) Image of recovered ρ values as determined by a linear fit to the vectorized form of equation (7). The process of vectorization is detailed in reference 9. Scale bar is 50 μm. B) The distribution of recovered ρ, with the mean value of 1.73 highlighted in orange.

The distribution of ρ recovered shows a large spread ($\sigma = 0.68$) across the field of view. This is consistent with the analytical approach taken, where few individual measurements at each pixel provide many low signal to noise measurements. The trade-off for this uncertainty is the ability to map the ratio ρ across the field of view on a per-pixel basis and low measurement time; a single frame obtained for this data analysis can be obtained at video rate; however, the limiting time factor in these measurements is the rotation of detection QWP and polarizer. The recovered mean value ρ = 1.73 is in excellent agreement with previously reported values of 1.69 for thin tissue segments analyzed with the depolarizer approach.[11] Furthermore, this number is consistent with previous nonlinear optical Stokes ellipsometry (NOSE) results and polarization in-polarization out (PIPO) studies by Tuer *et al*. where values near 1.4 were recovered for mouse tail tendon.[12, 13]

5. CONCLUSIONS

Local frame tensor information has been recovered for collagen embedded in thick turbid tissue sections. Two distinct experimental methods have been employed, the first relying on depolarization of the fundamental prior to entry to the turbid environment. The pre-depolarization approach minimizes the effects of the native tissue's turbidity on the polarization state of light prior to SHG, allowing the use of a predictive framework for expected SHG activity as function solely of collagen orientation and tensor elements. Resulting values for ρ yield a distribution with a mean value of 2.55, likely biased large due to the underlying probability distribution as a ratio of random numbers. It is posited that slight depolarization of the second harmonic on exiting the focal plane result in the deviation. The second method builds on the groundwork laid by pre-depolarization. Where the use of the depolarizer array enables the operation in the regime of fully depolarized light, allowing the verification of the Stokes-Mueller theoretical framework, the Mueller tensor approach operates in the regime of partial depolarization. Furthermore, by measuring the Stokes vector of both the fundamental and the second harmonic, any specific evaluation of the Mueller matrix representing depolarization of the fundamental by the turbid environment can be avoided. Instead the depolarization is implicit in the Stokes vector of the fundamental. We demonstrate the measurement of local frame tensor element magnitudes $\left|\chi_{VVV}\right|^2$ and $\left|\chi_{VHH}\right|^2$, recovering the tensor element ratio $\rho = \left|\chi_{VVV} / \chi_{VHH}\right|$ = 1.73 in excellent agreement with previous reports. This achievement demonstrates an important milestone in the pursuit of a nonlinear optical polarization dependent microscopy with arbitrary degree of depolarization. Future work will aim to use samples where the SHG-active substrate is embedded near the center of a depolarizing medium, such that significant depolarization of the fundamental and the second harmonic is expected.

6. ACKNOWLEDGEMENTS

The authors gratefully acknowledge support from the NIH Grant Numbers R01GM-103401 and R01GM-103910 from the NIGMS.

REFERENCES

[1] P. J. Campagnola, and L. M. Loew, "Second-harmonic imaging microscopy for visualizing biomolecular arrays in cells, tissues and organisms," Nature Biotechnology, 21(11), 1356-1360 (2003).

[2] S. Psilodimitrakopoulos, and S. Santos, "In vivo, pixel-resolution mapping of thick filaments' orientation in nonfibrilar muscle using polarization-sensitive second harmonic generation microscopy," … of biomedical optics, (2009).

[3] E. L. DeWalt, S. Z. Sullivan, P. D. Schmitt *et al.*, "Polarization-Modulated Second Harmonic Generation Ellipsometric Microscopy at Video Rate," Analytical Chemistry, 86(16), 8448-8456 (2014).

[4] K. Tilbury, C.-H. H. Lien, S.-J. J. Chen *et al.*, "Differentiation of Col I and Col III isoforms in stromal models of ovarian cancer by analysis of second harmonic generation polarization and emission directionality," Biophysical journal, 106(2), 354-365 (2014).

[5] X. Y. Dow, E. L. DeWalt, J. A. Newman *et al.*, "Unified Theory for Polarization Analysis in Second Harmonic and Sum Frequency Microscopy," Biophysical Journal, 111(7), 1553-1568 (2016).

[6] O. Nadiarnykh, and P. J. Campagnola, "Retention of polarization signatures in SHG microscopy of scattering tissues through optical clearing," Optics express, (2009).
[7] H. B. de Aguiar, S. Gigan, and S. Brasselet, "Polarization recovery through scattering media," Science Advances, (2017).
[8] S. Krouglov, B. Stewart, and V. Barzda, "Second harmonic generation double Stokes Mueller polarimetric microscopy of myofilaments," Biomedical optics …, (2016).
[9] G. J. Simpson, "Connection of Jones and Mueller Tensors in Second Harmonic Generation and Multi-Photon Fluorescence Measurements," The Journal of Physical Chemistry B, 120(13), 3281-3302 (2016).
[10] Y. Shi, W. M. McClain, and R. A. Harris, "Generalized Stokes-Mueller formalism for two-photon absorption, frequency doubling, and hyper-Raman scattering," Physical Review A, 49(3), 1999-2015 (1994).
[11] C. U. Ding, James RW; Deng, Fengyuang; Simpson, Garth J, "Second Harmonic Generation of Unpolarized Light," Physical Review Letters, Accepted, (2017).
[12] A. E. Tuer, S. Krouglov, N. Prent *et al.*, "Nonlinear Optical Properties of Type I Collagen Fibers Studied by Polarization Dependent Second Harmonic Generation Microscopy," The Journal of Physical Chemistry B, 115(44), 12759-12769 (2011).
[13] X. Y. Dow, E. L. DeWalt, S. Z. Sullivan *et al.*, "Imaging the Nonlinear Susceptibility Tensor of Collagen by Nonlinear Optical Stokes Ellipsometry," Biophysical Journal, 111(7), 1361-1374 (2016).
[14] W. S. Rasband, [ImageJ] National Institutes of Health, (1997-2016).
[15] O. Nadiarnykh, S. Plotnikov, W. A. Mohler *et al.*, "Second harmonic generation imaging microscopy studies of osteogenesis imperfecta," Journal of biomedical optics, 12(5), 51805 (2007).